- Supplementary Information -

Pyrrolic FeN_4 models for FeNC catalysts: the influence of planarity on electronic properties and Mössbauer parameters

Niklas von Rhein[1‡], Jian Liang Low[2‡], Charlotte Gallenkamp[1], Beate Paulus[2] and Vera Krewald[1]

[1] TU Darmstadt, Department of Chemistry, Quantum Chemistry, Peter-Grünberg-Straße 4, 64287 Darmstadt, Germany
[2] FU Berlin, Physical and Theoretical Chemistry, Arnimallee 22, 14195 Berlin, Germany
‡ Authors contributed equally to this work

Table of contents

- DFT Data (Supplementary Tables S1 – S4) -

Supplementary Table S1: Overview over energy data and Mulliken spin populations calculated with DFT. The multiplicity, the final single point energy (FSPE) and the Mulliken spin population for the geometry optimization with TPSS functional, the single point calculation with OLYP or OPBE functional and the Mössbauer parameter calculation with the B3LYP functional as well as the relative spin state energy for the single point calculation are shown. The models **1** to **3** are named analogously to the main text. Single point calculations are performed with OLYP functional for model **3** and with OPBE functional for model **1** and **2**.

		Geo-Opt (TPSS)		Single Point (OLYP/OPBE)			Mössbauer (B3LYP)	
	M	*FSPE* / Ha	Mull (Fe)	*FSPE* / Ha	E_{Rel} / kcal mol^{-1}	Mull (Fe)	*FSPE* / Ha	Mull (Fe)
1	1	-3475.5211	2.32	-3476.5342	23.1	1.91	-3476.0982	1.97
	3	-3475.5164	2.26	-3476.5710	0.0	2.47	-3476.0923	2.29
	5	-3475.5134	2.17	-3476.5551	10.0	1.90	-3476.0985	1.97
1 (extended)	1[a]	—	—	—	—	—	—	—
	3	-5154.3040	2.30	-5155.8756	0.0	2.55	-5155.2682	2.37
	5	-5154.2984	2.41	-5155.8713	2.7	2.61	-5155.2676	2.31
1*O2	1	-3625.7731	1.07	-3626.8917	6.7	1.76	-3626.4316	-1.25
	3	-3625.7770	-1.20	-3626.9023	0.0	-1.14	-3626.4347	-1.28
	5	-3625.7656	1.37	-3626.8931	5.8	1.78	-3626.4316	2.56
1*OH	2	-3551.2841	1.04	-3552.3779	0.0	-1.21	-3551.9166	-0.96
	4	-3551.2834	0.96	-3552.3726	3.3	1.16	-3551.9124	0.95
1*H2O	1	-3551.9114	2.41	-3553.0148	0.0	2.59	-3552.5513	2.69
	3	-3551.9054	2.42	-3553.0094	3.4	2.61	-3552.5452	2.68
	5	-3551.9023	2.44	-3553.0062	5.4	2.65	-3552.5431	2.72
1*2 O2	1	-3776.0174	-0.99	-3777.2147	1.3	-1.42	-3776.7752	-1.10
	3	-3776.0182	-0.77	-3777.2148	1.2	-1.47	-3776.7739	-1.17
	5	-3776.0215	-0.82	-3777.2167	0.0	-0.57	-3776.7575	-1.11
	7	-3776.0106	0.82	-3777.2050	7.3	0.99	-3776.7510	1.31
1*2 OH	1	-3627.0517	-1.40	-3628.1891	0.0	1.38	-3627.7464	1.02
	3	-3627.0493	1.50	-3628.1852	2.4	1.59	-3627.7397	0.99
	5	-3627.0487	1.56	-3628.1821	4.4	1.77	-3627.7282	1.88
1*2 H2O	1	-3628.2886	0.47	-3629.4202	8.8	0.00	-3628.9649	0.00
	3	-3628.2904	-0.39	-3629.4164	11.2	-0.22	-3628.9797	-0.27
	5	-3628.2907	2.50	-3629.4342	0.0	2.69	-3628.9914	2.78
	7	-3628.2893	2.63	-3629.4321	1.3	2.81	-3628.9929	2.85
2	1	-3475.5119	2.05	-3476.5519	12.8	1.82	-3476.1002	1.95
	3	-3475.5272	2.16	-3476.5723	0.0	2.38	-3476.1168	2.17
	5	-3475.4994	3.70	-3476.5538	11.6	3.88	-3476.1084	3.73
2 (extended)	1[b]	-5154.2749	-1.96	-5155.8449	1.9	2.64	-5155.2488	2.21
	3	-5154.2772	2.33	-5155.8479	0.0	2.66	-5155.2485	2.22
	5	-5154.2764	2.34	-5155.8450	1.8	2.65	-5155.2497	2.22
2*O2	1	-3625.7870	1.13	-3626.9040	1.3	0.00	-3626.4293	0.00
	3	-3625.7807	1.63	-3626.9100	0.0	1.91	-3626.4493	2.12
(end-on)	5	-3625.7711	1.13	-3626.9011	3.0	2.57	-3626.4562	2.52
(side-on)	5	-3625.7728	2.48	-3626.9010	3.2	2.66	-3626.4553	2.67

		Geo-Opt (TPSS)		Single Point (OLYP/OPBE)			Mössbauer (B3LYP)	
	M	*FSPE* / Ha	Mull (Fe)	*FSPE* / Ha	E_{Rel} / kcal mol^{-1}	Mull (Fe)	*FSPE* / Ha	Mull (Fe)
2*OH	2	-3551.3018	0.92	-3552.3870	3.9	1.15	-3551.9391	1.03
	4	-3551.2943	2.58	-3552.3932	0.0	2.78	-3551.9482	2.79
2*H2O	1	-3551.9011	2.09	-3552.9815	18.7	0.00	-3552.5344	0.00
	3	-3551.9162	2.16	-3553.0113	0.0	2.41	-3552.5656	2.15
	5	-3551.8931	2.20	-3552.9892	13.9	2.49	-3552.5435	2.15
2*2 O2	1	-3776.0326	-0.82	-3777.2316	0.4	-1.01	-3776.8128	-1.09
	3	-3776.0374	-1.04	-3777.2322	0.0	-1.09	-3776.8120	-1.13
	5	-3776.0326	0.40	-3777.2320	0.1	0.79	-3776.8008	1.07
2*2 OH	1	-3627.0606	0.31	-3628.1952	2.7	-1.24	-3627.7697	-1.01
	3	-3627.0699	1.48	-3628.1995	0.0	1.54	-3627.7680	1.00
	5	-3627.0477	1.59	-3628.1760	14.8	1.82	-3627.7296	1.92
2*2 H2O	1	-3628.3040	0.00	-3629.3953	27.9	2.74	-3628.9596	2.36
	3	-3628.2981	2.19	-3629.4397	0.0	2.46	-3629.0102	2.15
	5	-3628.2763	2.26	-3629.4185	13.3	2.56	-3628.9884	2.14
3	1	-3398.5172	0.00	-3399.3287	36.5	0.00	-3398.6575	0.00
	3	-3398.5763	1.97	-3399.3870	0.0	1.88	-3398.7318	1.95
	5	-3398.5403	2.62	-3399.3614	16.0	2.67	-3398.6830	2.84
3 (extended)	1	-5002.3496	0.00	-5003.6723	64.8	0.00	-5002.8574	0.00
	3	-5002.3908	1.96	-5003.7756	0.0	1.86	-5002.9174	1.95
	5	-5002.2403	3.68	-5003.7091	41.7	3.75	-5002.8827	2.86
3*O2 (end-on)	1	-3549.0125	0.00	-3549.7618	4.9	0.00	-3549.0387	0.00
	3	-3549.0143	1.83	-3549.7675	1.4	2.00	-3549.0516	1.48
	5	-3549.0125	2.51	-3549.7697	0.0	2.52	-3549.0788	2.68
(side-on)	1	-3549.0142	0.00	-3549.7655	2.6	0.00	-3549.0396	0.00
	3	-3549.0172	1.64	-3549.7645	3.3	1.77	-3549.0565	2.19
	5	-3549.0065	2.56	-3549.7654	2.7	2.63	-3549.0679	2.69
3*OH	2	-3474.4414	0.92	-3475.2125	15.4	0.92	-3474.5449	1.00
	4	-3474.4517	2.61	-3475.2370	0.1	2.68	-3474.5690	2.77
	6	-3474.4362	4.10	-3475.2371	0.0	4.14	-3474.5692	4.25
3*H2O	1	-3475.0339	0.00	-3475.8036	15.1	0.00	-3475.1449	0.00
	3	-3475.0564	2.10	-3475.8276	0.0	2.24	-3475.1737	2.12
	5	-3475.0329	2.63	-3475.8275	0.1	3.80	-3475.1723	3.80
	5	-3475.0311	3.70	-3475.8168	6.8	2.70	-3475.1438	2.84
3*2 H2O	1	-3552.0000	0.00	-3552.2577	0.8	0.00	-3551.6008	0.00
	3	-3551.5107	0.84	-3552.2343	15.5	0.82	-3551.5715	0.98
	5	-3551.5134	2.67	-3552.2590	0.0	2.72	-3551.5924	2.86

[a] No geometry convergence could be reached, an imaginary mode of over 500 cm^{-1} was observed.
[b] No frequency calculation could be performed; thus it could not be verified that the structure is a local minimum.

Supplementary Table S2: Mulliken spin populations of the model complexes. The Mulliken spin populations are calculated with the B3LYP functional for all models.

	M	Fe	∑ (N)	∑ (Ring)	∑ (Axial Ligands)
1	1	1.97	-0.21	-1.76	—
	3	2.29	-0.18	-0.11	—
	5	1.97	-0.20	2.23	—
1 (extended)	1	—	—	—	—
	3	2.40	-0.18	-0.22	—
	5	2.42	-0.04	1.61	—
1*O2	1	-1.25	0.12	-0.06	1.20
	3	-1.28	0.09	1.98	1.20
	5	2.56	-0.17	2.18	-0.57
1*OH	2	-0.96	0.06	1.97	-0.07
	4	0.95	-0.06	2.03	0.08
1*H2O	1	2.69	-0.17	-2.56	0.04
	3	2.68	-0.14	-0.58	0.04
	5	2.72	-0.13	1.37	0.04
1*2 O2	1	-1.10	0.03	1.04	0.02
	3	-1.17	0.03	1.09	2.05
	5	-1.11	0.23	2.78	2.10
	7	1.31	0.02	2.80	1.87
1*2 OH	1	1.02	0.01	-1.15	0.12
	3	0.99	-0.21	1.14	0.08
	5	1.88	-0.20	2.14	0.19
1*2 H2O	1	0.00	0.00	0.00	0.00
	3	-0.27	-0.01	2.31	-0.02
	5	2.78	-0.14	1.29	0.07
	7	2.85	-0.09	3.20	0.05
2	1	1.95	-0.24	-1.72	—
	3	2.17	-0.23	0.06	—
	5	3.73	0.09	0.18	—
2 (extended)	1	2.14	-0.19	-1.95	—
	3	2.22	-0.20	-0.02	—
	5	2.22	-0.24	2.01	—
2*O2	1	0.00	0.00	0.00	0.00
	3	2.10	-0.22	-0.82	0.94
(end-on)	5	2.67	-0.16	0.11	1.38
(side-on)	5	2.52	-0.22	0.19	1.51
2*OH	2	1.03	-0.10	0.03	0.04
	4	2.79	-0.17	0.12	0.26
2*H2O	1	0.00	0.00	0.00	0.00
	3	2.15	-0.19	0.02	0.02
	5	2.15	-0.11	1.94	0.02
2*2 O2	1	-1.09	0.11	-1.01	1.99
	3	-1.13	0.14	0.96	2.03
	5	1.07	-0.10	1.05	1.98

	M	Fe	∑ (N)	∑ (Ring)	∑ (Axial Ligands)
2*2 OH	1	-1.01	0.13	0.96	-0.07
	3	1.00	-0.08	0.99	0.08
	5	1.92	-0.14	1.99	0.24
2*2 H2O	1	2.36	-0.18	-2.27	0.09
	3	2.15	-0.15	-0.04	0.04
	5	2.14	-0.05	1.87	0.04
3	1	0.00	0.00	0.00	—
	3	1.95	-0.16	0.21	—
	5	2.84	-0.21	1.37	—
3 (extended)	1	0.00	0.00	0.00	—
	3	1.95	-0.16	0.21	—
	5	2.86	-0.20	1.34	—
3*O2 (end-on)	1	0.00	0.00	0.00	0.00
	3	1.48	-0.09	0.05	0.56
	5	2.68	-0.18	0.25	1.25
(side-on)	1	0.00	0.00	0.00	0.00
	3	2.19	-0.12	0.17	-0.25
	5	2.69	-0.14	0.16	1.30
3*OH	2	1.00	-0.09	0.08	0.02
	4	2.77	-0.17	0.18	0.22
	6	4.25	0.28	0.23	0.24
3*H2O	1	2.84	-0.23	1.34	0.05
	3	0.00	0.00	0.00	0.00
	5	2.12	-0.15	0.01	0.02
	5	3.80	0.02	0.15	0.02
3*2 H2O	1	0.00	0.00	0.00	0.00
	3	0.98	-0.18	1.22	-0.02
	5	2.86	-0.22	1.30	0.07

Supplementary Table S3: Selected structural data of the model complexes. The *trans*-N-Fe-N angle is averaged over both angles. The out of plane (OOP) character is calculated by creating a plane through all four nitrogen atoms using the program ChimeraX and then calculating the iron-plane distance.

		Atom-Atom-Distances / Å							*trans*-	OOP
	M	Fe-N_1	Fe-N_2	Fe-N_3	Fe-N_4	Fe-N (av)	Fe-O_1	Fe-O_2	N-Fe-N / °	/ Å
1	1	1.954	1.954	1.954	1.954	1.954	—	—	180.0	0.000
	3	1.957	1.956	1.956	1.957	1.956	—	—	180.0	0.000
	5	1.959	1.960	1.959	1.960	1.960	—	—	180.0	0.000
1 (extended)	1	—	—	—	—	—	—	—	—	—
	3	1.955	1.956	1.955	1.956	1.956	—	—	180.0	0.000
	5	1.958	1.958	1.958	1.958	1.958	—	—	180.0	0.000
1*O2	1	1.969	1.959	1.960	1.969	1.964	1.826	—	170.0	0.171
	3	1.957	1.965	1.965	1.957	1.961	1.844	—	170.5	0.163
	5	1.965	1.970	1.970	1.965	1.967	1.845	—	169.5	0.181
1*OH	2	1.967	1.963	1.967	1.961	1.964	1.771	—	168.3	0.201
	4	1.970	1.965	1.970	1.961	1.967	1.768	—	168.1	0.204
1*H2O	1	1.953	1.959	1.967	1.958	1.959	2.235	—	175.5	0.077
	3	1.955	1.961	1.969	1.958	1.960	2.229	—	175.2	0.081
	5	1.954	1.965	1.968	1.964	1.963	2.236	—	175.2	0.082
1*2 O2	1	1.978	1.978	1.963	1.963	1.971	1.930	1.931	179.7	0.002
	3	1.961	1.969	1.962	1.963	1.964	1.913	1.959	179.7	0.005
	5	1.962	1.962	1.962	1.962	1.962	1.969	1.969	180.0	0.000
	7	1.967	1.970	1.966	1.968	1.968	1.958	1.959	179.9	0.001
1*2 OH	1	1.965	1.989	1.965	1.989	1.977	1.835	1.835	179.9	0.000
	3	1.986	1.986	1.977	1.977	1.981	1.820	1.820	177.7	0.002
	5	1.992	1.992	1.977	1.977	1.984	1.812	1.813	177.4	0.002
1*2 H2O	1	1.966	1.964	1.966	1.964	1.965	2.016	2.016	179.9	0.001
	3	1.973	1.974	1.973	1.974	1.973	2.175	2.176	180.0	0.000
	5	1.966	1.973	1.966	1.974	1.970	2.310	2.312	180.0	0.000
	7	1.972	1.972	1.972	1.972	1.972	2.299	2.300	180.0	0.000
2	1	1.971	1.972	1.972	1.970	1.971	—	—	176.7	0.013
	3	1.973	1.973	1.973	1.973	1.973	—	—	176.8	0.014
	5	2.065	2.066	2.066	2.066	2.066	—	—	177.7	0.002
2 (extended)	1	2.000	2.000	2.000	2.000	2.000	—	—	179.9	0.001
	3	1.997	1.998	1.998	1.999	1.998	—	—	179.7	0.005
	5	1.998	1.999	1.998	1.999	1.999	—	—	179.7	0.006
2*O2	1	1.975	1.980	1.985	1.973	1.978	1.815	—	169.3	0.184
	3	1.982	1.980	1.984	1.980	1.982	1.855	—	169.6	0.180
(end-on)	5	1.982	1.980	1.981	1.976	1.980	2.273	—	174.8	0.089
(side-on)	5	2.009	1.978	2.009	1.978	1.993	2.176	—	165.3	0.255
2*OH	2	1.978	1.971	1.974	1.970	1.973	1.778	—	169.4	0.182
	4	2.008	1.987	2.010	1.990	1.999	1.855	—	163.6	0.285
2*H2O	1	1.978	1.976	1.968	1.968	1.973	2.256	—	175.8	0.072
	3	1.986	1.981	1.975	1.972	1.979	2.265	—	175.4	0.080
	5	1.990	1.983	1.976	1.976	1.981	2.267	—	175.9	0.070

		Atom-Atom-Distances / Å							*trans*-	OOP
	M	**Fe-N_1**	**Fe-N_2**	**Fe-N_3**	**Fe-N_4**	**Fe-N (av)**	**Fe-O_1**	**Fe-O_2**	**N-Fe-N / °**	**/ Å**
2*2 O2	1	1.987	1.981	1.984	1.985	1.984	1.883	1.907	178.3	0.005
	3	1.986	1.983	1.986	1.985	1.985	1.916	1.925	178.3	0.002
	5	1.981	1.977	1.974	1.978	1.977	1.919	1.946	178.4	0.003
2*2 OH	1	1.966	1.989	2.007	1.993	1.989	1.814	1.835	177.6	0.007
	3	1.970	2.000	2.007	1.985	1.991	1.810	1.812	177.5	0.001
	5	1.987	2.001	2.002	1.991	1.995	1.806	1.806	176.9	0.001
2*2 H2O	1	1.974	1.976	1.975	1.974	1.975	2.016	2.016	177.9	0.001
	3	1.976	1.985	1.999	1.989	1.987	2.340	2.372	177.1	0.007
	5	1.975	1.990	2.003	1.987	1.989	2.328	2.373	177.3	0.013
3	1	1.896	1.896	1.896	1.896	1.896	—	—	174.2	0.096
	3	1.911	1.911	1.911	1.911	1.911	—	—	173.9	0.102
	5	1.900	1.900	1.900	1.900	1.900	—	—	174.0	0.099
3 (extended)	1	1.873	1.872	1.872	1.873	1.872	—	—	171.9	0.132
	3	1.905	1.905	1.905	1.905	1.905	—	—	172.8	0.120
	5	1.893	1.893	1.894	1.893	1.893	—	—	173.3	0.111
3*O2 (end-on)	1	1.994	1.967	1.967	1.993	1.980	1.721	—	156.8	0.399
	3	1.979	1.956	1.956	1.979	1.968	1.836	—	157.2	0.388
	5	1.924	1.922	1.922	1.923	1.923	2.125	—	162.9	0.286
(side-on)	1	1.937	1.919	1.921	1.936	1.928	1.716	—	160.4	0.328
	3	1.931	1.956	1.975	1.948	1.953	1.798	—	147.5	0.545
	5	1.959	1.934	1.958	1.934	1.946	2.113	—	154.5	0.430
3*OH	2	1.975	1.966	1.967	1.974	1.970	1.831	—	161.1	0.323
	4	1.966	1.963	1.961	1.968	1.964	1.928	—	153.7	0.447
	6	2.051	2.050	2.047	2.053	2.050	1.861	—	140.8	0.688
3*H2O	1	1.936	1.936	1.935	1.935	1.936	2.033	—	169.1	0.184
	3	1.923	1.925	1.925	1.923	1.924	2.250	—	166.9	0.220
	5	2.069	2.067	2.066	2.066	2.067	2.083	—	141.6	0.679
	5	1.916	1.915	1.916	1.915	1.915	2.159	—	165.8	0.237
3*2 H2O	1	1.922	1.922	1.922	1.922	1.922	2.023	2.038	175.8	0.070
	3	1.925	1.925	1.925	1.925	1.925	1.977	1.998	177.3	0.045
	5	1.918	1.920	1.921	1.920	1.920	2.284	2.384	174.2	0.097

Supplementary Table S4: Mössbauer data of all spin states of the model complexes. The relative spin state energy, the Mulliken spin population on the iron atom, the *s*-electron density, the isomer shift and the quadrupole splitting are given. The relative energy is calculated using the OPBE/OLYP functional (see also supplementary table S1), the Mössbauer data using the B3LYP functional.

	M	E_{Rel} / kcal mol^{-1}	Mull (Fe)	ρ / au^{-3}	δ_{iso} / mm s^{-1}	ΔE_q / mm s^{-1}
1	1	23.1	1.97	11816.81269	0.428	0.703
	3	0.0	2.29	11816.57794	0.548	1.878
	5	10.0	1.97	11816.78679	0.441	0.677
1 (extended)	1	—	—	—	—	—
	3	0.0	2.40	11816.66290	0.505	2.415
	5	2.7	2.42	11816.65997	0.506	2.414
1*O2	1	6.7	-1.25	11816.93343	0.366	2.869
	3	0.0	-1.28	11816.91396	0.376	2.870
	5	5.8	2.56	11816.99391	0.336	2.495
1*OH	2	0.0	-0.96	11817.10675	0.278	-3.608
	4	3.3	0.95	11817.09175	0.286	-3.490
1*H2O	1	0.0	2.69	11816.79841	0.435	3.271
	3	3.4	2.68	11816.77766	0.446	3.242
	5	5.4	2.72	11816.80232	0.433	3.356
1*2 O2	1	1.3	-1.10	11816.92559	0.370	-2.234
	3	1.2	-1.17	11816.93357	0.366	-2.697
	5	0.0	-1.11	11816.93369	0.366	-2.316
	7	7.3	1.31	11817.01525	0.325	-2.468
1*2 OH	1	0.0	1.02	11817.10310	0.280	-2.614
	3	2.4	0.99	11817.08797	0.288	1.977
	5	4.4	1.88	11817.69272	-0.021	1.648
1*2 H2O	1	8.8	0.00	11816.32963	0.675	2.109
	3	11.2	-0.27	11816.26317	0.709	2.501
	5	0.0	2.78	11816.76458	0.453	3.066

	M	E_{Rel} / kcal mol^{-1}	Mull (Fe)	ρ / au^{-3}	δ_{iso} / mm s^{-1}	ΔE_q / mm s^{-1}
	7	1.3	2.85	11816.80455	0.432	3.199
2	1	12.8	1.95	11816.72417	0.473	0.576
	3	0.0	2.17	11816.43375	0.621	1.354
	5	11.6	3.73	11816.22677	0.727	-0.297
2 (extended)	1	1.9	2.21	11816.25419	0.713	1.197
	3	0.0	2.22	11816.31086	0.684	1.321
	5	1.8	2.22	11816.30572	0.687	1.316
2*O2	1	1.3	0.00	11816.80988	0.430	2.519
	3	0.0	2.12	11816.57897	0.547	-1.575
(end-on)	5	3.0	2.52	11816.79206	0.439	1.962
(side-on)	5	3.2	2.67	11816.57392	0.550	2.846
2*OH	2	3.9	1.03	11817.05217	0.306	-2.664
	4	0.0	2.79	11816.92162	0.373	1.383
2*H2O	1	18.7	0.00	11816.00308	0.841	3.768
	3	0.0	2.15	11816.28144	0.699	-1.416
	5	13.9	2.15	11816.26034	0.710	-1.431
2*2 O2	1	0.4	-1.09	11816.93510	0.366	-2.090
	3	0.0	-1.13	11816.88562	0.391	-2.133
	5	0.1	1.07	11816.91365	0.377	-2.512
2*2 OH	1	2.7	-1.01	11817.05735	0.303	2.365
	3	0.0	1.00	11817.07138	0.296	2.337
	5	14.8	1.92	11817.69969	-0.025	1.620
2*2 H2O	1	27.9	2.36	11816.38968	0.644	-0.980
	3	0.0	2.15	11816.17086	0.756	-1.607
	5	13.3	2.14	11816.14754	0.768	-1.564
3	1	36.5	0.00	11817.29541	0.182	-5.951
	3	0.0	1.95	11817.0410	0.312	1.149

	M	E_{Rel} / kcal mol^{-1}	Mull (Fe)	ρ / au^{-3}	δ_{iso} / mm s^{-1}	ΔE_q / mm s^{-1}
				6		
	5	16.0	2.84	11817.18165	0.240	4.846
3 (extended)	1	64.8	0.00	11817.36472	0.146	-5.308
	3	0.0	1.95	11817.07541	0.294	1.226
	5	41.7	2.86	11817.21958	0.220	4.665
3*O2 (end-on)	1	4.9	0.00	11817.18387	0.239	-2.615
	3	1.4	1.48	11817.00180	0.332	-3.056
	5	0.0	2.68	11817.08345	0.290	2.694
3*O2 (side-on)	1	2.6	0.00	11817.40266	0.127	3.000
	3	3.3	2.19	11817.15511	0.253	2.188
	5	2.7	2.69	11816.73269	0.469	2.686
3*OH	2	15.4	1.00	11817.03210	0.316	2.513
	4	0.1	2.77	11816.97816	0.344	1.541
	6	0.0	4.25	11816.81384	0.428	-0.437
3*H2O	1	15.1	0.00	11816.19902	0.741	3.319
	3	0.0	2.12	11816.48619	0.595	-2.104
	5	0.1	3.80	11815.56606	1.064	4.832
	5	6.8	2.84	11817.07812	0.293	3.720
3*2 H2O	1	0.8	0.00	11816.30620	0.687	2.236
	3	15.5	0.98	11816.91632	0.375	3.305
	5	0.0	2.86	11817.02548	0.320	3.763

- Orbital Occupation (Supplementary Table S5 - and Figures S1 – S6)

Supplementary Table S5: Occupation of the orbitals used for calculating the conjugation. All occupied orbitals with an iron-*d*-character of 15 % or more are shown for the models without axial ligands. The orbital number MO is given together with its character (α or β). ∑p/d means that the sum of the orbital occupation over all p/d-orbitals for the given atoms is shown. ∑C,N means that all carbon and nitrogen atoms are viewed, ∑C that all carbon atoms are viewed.

	M		d_{xy} (Fe)	d_{xz} (Fe)	d_{yz} (Fe)	$d_{x^2-y^2}$ (Fe)	d_{z^2} (Fe)	p_z (∑C,N)	p_z (∑C)	∑d (Fe)	∑p (∑C,N)	∑p (∑C)
	174	α	0.0	11.7	39.7	0.1	0.0	41.4	38.1	51.5	41.4	38.1
	176	α	0.0	15.0	4.1	0.0	0.1	69.0	62.7	19.2	69.0	62.7
	179	α	33.5	0.4	0.2	3.6	44.8	0.0	0.0	82.5	7.8	3.2
	183	α	0.1	22.7	5.8	0.0	0.2	59.8	58.7	28.8	59.8	58.7
1	184	α	45.0	0.0	0.0	4.9	36.0	0.0	0.0	85.9	5.1	2.1
	187	α	0.0	20.0	6.5	0.0	0.2	58.5	46.2	26.7	58.5	46.2
	184	β	69.6	0.0	0.0	7.7	12.0	0.0	0.0	89.3	3.4	1.8
	187	β	0.0	22.1	9.4	0.0	0.2	52.4	51.8	31.7	52.4	51.8
	190	β	0.0	19.8	8.7	0.0	0.2	53.8	51.2	28.7	53.8	51.2
	297	α	0.0	24.2	16.8	0.0	0.2	49.6	48.6	41.2	49.6	48.6
	300	α	23.3	0.2	0.0	2.4	49.5	0.0	0.0	75.4	11.0	4.6
	301	α	0.0	13.3	17.4	0.0	0.1	57.8	57.4	30.8	57.8	57.4
1 (extended)	307	α	51.4	0.3	0.1	5.5	27.3	0.0	0.0	84.6	6.4	3.0
	314	β	71.7	0.2	0.1	7.5	9.7	0.0	0.0	89.2	3.6	2.2
	318	β	0.0	6.6	10.3	0.0	0.0	63.8	63.4	16.9	63.8	63.4
	323	β	0.0	12.9	20.8	0.0	0.0	49.8	49.2	33.7	49.8	49.2
	175	α	0.0	26.8	17.3	0.0	0.2	39.8	36.7	44.3	45.3	41.1
	177	α	0.0	13.1	8.4	0.0	0.1	57.3	57.3	21.6	63.9	63.9
	178	α	48.3	0.0	0.1	2.7	27.5	7.4	5.3	78.6	12.2	7.6
	179	α	0.2	12.6	20.1	0.1	0.1	49.6	41.1	33.1	54.5	44.8
	182	α	4.1	0.2	0.0	0.3	31.1	42.2	33.3	35.7	48.1	37.0
2	184	α	27.2	0.1	0.1	1.5	18.3	33.3	28.5	47.2	39.6	32.7
	186	α	0.0	11.2	6.9	0.0	0.1	60.7	45.5	18.2	66.3	50.0
	189	α	0.0	14.2	23.3	0.0	0.0	45.1	37.8	37.5	49.1	41.3
	186	β	57.1	0.1	0.1	3.5	11.4	13.9	13.3	72.2	17.4	15.8
	190	β	0.0	21.7	35.1	0.1	0.0	29.3	24.9	56.9	31.9	27.3
	298	α	0.0	23.0	13.7	0.0	0.1	52.2	51.5	36.8	52.2	51.5
	301	α	0.0	11.0	4.3	0.0	0.1	70.3	70.1	15.4	70.3	70.1
	303	α	43.2	0.0	0.0	2.2	39.4	0.0	0.0	84.8	6.6	2.9
	304	α	0.0	9.6	15.3	0.0	0.0	62.1	58.5	24.9	62.1	58.5
2 (extended)	306	α	0.0	6.7	13.8	0.0	0.0	64.8	64.0	20.5	64.8	64.0
	309	α	41.4	0.2	0.1	2.2	42.9	0.0	0.0	86.8	5.0	2.0
	316	α	0.0	6.3	14.7	0.0	0.0	62.8	57.5	21.0	62.8	57.5
	317	β	73.5	0.1	0.1	4.1	12.6	0.0	0.0	90.4	2.9	1.7
	322	β	0.0	14.7	20.9	0.0	0.0	48.2	44.9	35.6	48.2	44.9

	M		d_{xy} (Fe)	d_{xz} (Fe)	d_{yz} (Fe)	$d_{x^2-y^2}$ (Fe)	d_{z^2} (Fe)	p_z (∑C,N)	p_z (∑C)	∑d (Fe)	∑p (∑C,N)	∑p (∑C)
	169	α	0.0	15.1	15.4	0.0	0.0	55.6	51.2	30.5	58.8	54.4
	170	α	0.0	27.5	26.9	0.0	0.0	33.8	29.8	54.4	36.2	32.2
	177	α	85.2	0.0	0.0	0.0	3.5	1.2	0.8	88.7	4.8	3.2
	179	α	0.0	13.7	13.4	0.0	0.0	55.6	48.0	27.1	59.6	51.6
3	180	α	0.0	16.3	16.6	0.0	0.0	49.4	34.5	32.9	51.8	36.1
	181	α	1.2	0.0	0.0	0.0	51.2	28.4	28.0	52.4	32.8	30.0
	182	α	1.9	0.0	0.0	0.0	27.8	47.1	46.3	29.7	52.1	50.1
	180	β	81.9	0.0	0.0	0.0	7.2	1.2	1.2	89.1	4.8	4.0
	184	β	6.8	0.0	0.0	0.0	74.9	0.3	0.1	81.7	4.7	2.1
	290	α	0.0	0.0	17.7	0.0	0.0	63.8	62.2	17.7	65.8	64.2
	292	α	0.0	24.3	0.0	0.0	0.0	57.6	56.8	24.3	59.2	58.4
	293	α	0.0	0.0	36.4	0.0	0.0	47.4	46.6	36.4	49.0	48.2
	301	α	0.0	0.0	0.0	84.2	4.3	1.2	0.8	88.5	4.4	3.2
	304	α	0.0	0.0	21.5	0.0	0.0	58.4	53.6	21.5	61.2	55.6
3 (extended)	305	α	0.0	28.1	0.0	0.0	0.0	53.0	42.2	28.1	55.0	43.4
	308	α	0.0	0.0	0.0	2.6	65.3	12.0	11.2	67.9	17.8	13.0
	309	α	0.0	0.0	0.0	0.8	13.4	60.2	50.6	14.2	62.4	52.8
	307	β	0.0	0.0	0.0	81.2	8.6	0.0	0.0	89.8	2.8	2.0
	311	β	0.0	0.0	0.0	8.0	74.1	0.4	0.0	82.1	5.2	2.0

Supplementary Figures S1 – S6: Selected d-orbitals of the free and extended models. In the supplementary figures S1 to S6, the occupied iron-β-d_{xy}-orbitals of the models **1**, $\mathbf{1}_{\text{Large}}$, **2**, $\mathbf{2}_{\text{Large}}$ and **3** together with the occupied iron-β-$d_{x^2y^2}$-orbital of model $\mathbf{3}_{\text{Large}}$ are shown to illustrate the different hybridization of the iron-*d*-orbitals with the p_z-orbitals of the π-system depending on the system's planarity. For model $\mathbf{3}_{\text{Large}}$, the iron-$d_{x^2y^2}$-orbital is occupied instead of the iron-d_{xy}-orbital.

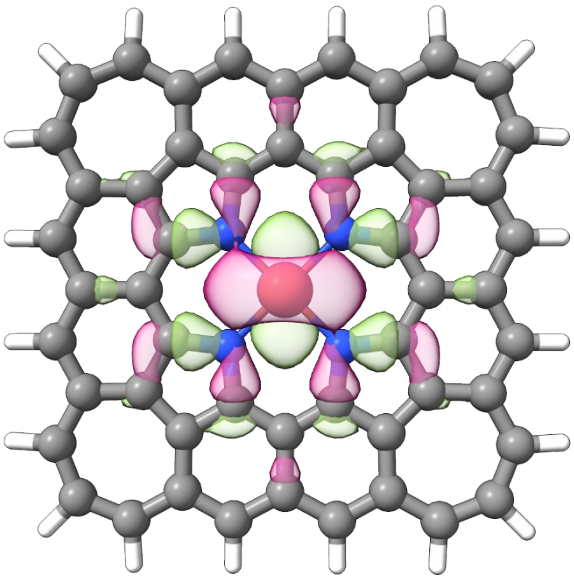

Figure S1: Iron-d_{xy}-orbital of model **1**. β-orbital 187 in ORCA nomenclature is shown. No hybridization with the p_z-orbitals of the π-system can be observed.

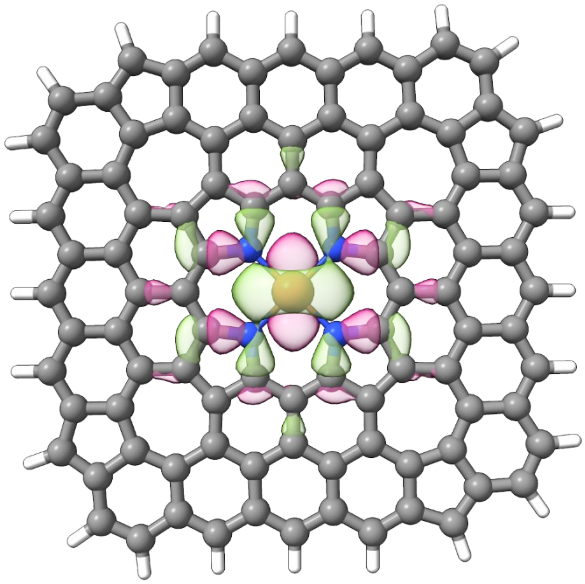

Figure S2: Iron-d_{xy}-orbital of model $\mathbf{1}_{\text{Large}}$. β-orbital 314 in ORCA nomenclature is shown. No hybridization with the p_z-orbitals of the π-system can be observed.

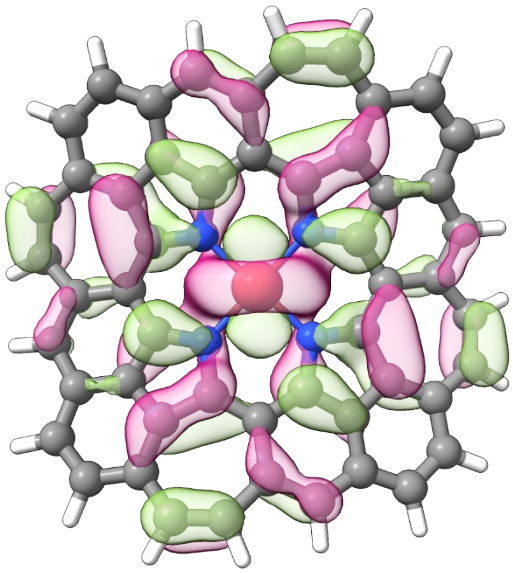

Figure S3: Iron-d_{xy}-orbital of model **2**. β-orbital 190 in ORCA nomenclature is shown. Strong hybridization with the p_z-orbitals of the π-system can be observed.

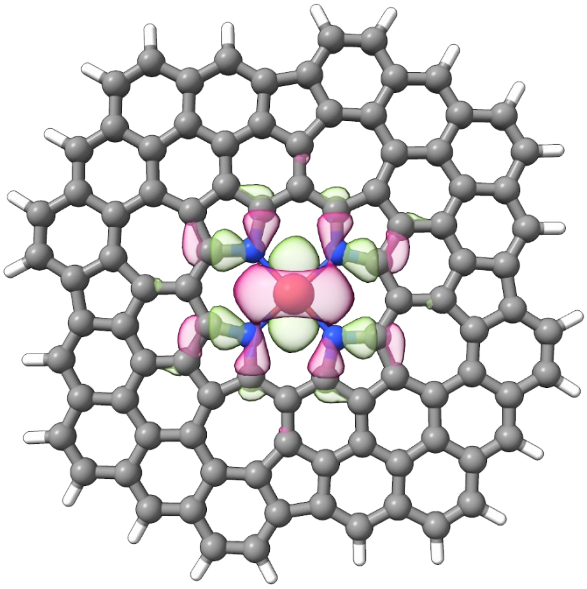

Figure S4: Iron-d_{xy}-orbital of model $\mathbf{2}_{\text{Large}}$. β-orbital 322 in ORCA nomenclature is shown. No hybridization with the p_z-orbitals of the π-system can be observed.

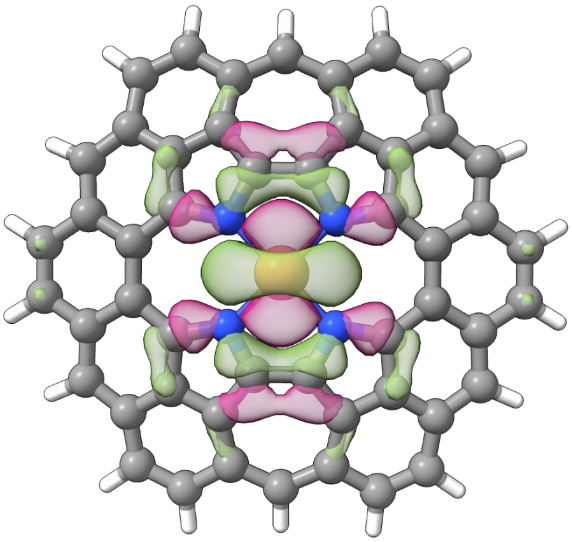

Figure S5: Iron-d_{xy}-orbital of model **3**. β-orbital 184 in ORCA nomenclature is shown. Weak hybridization with the p_z-orbitals of the π-system can be observed.

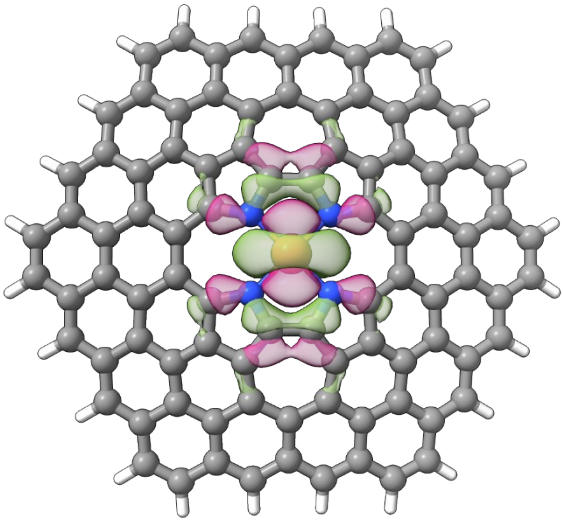

Figure S6: Iron-d_{xy}-orbital of model **3**. β-orbital 184 in ORCA nomenclature is shown. No hybridization with the p_z-orbitals of the π-system can be observed.

- Literature Mössbauer Data (Supplementary Table S6 - and Figure S7)

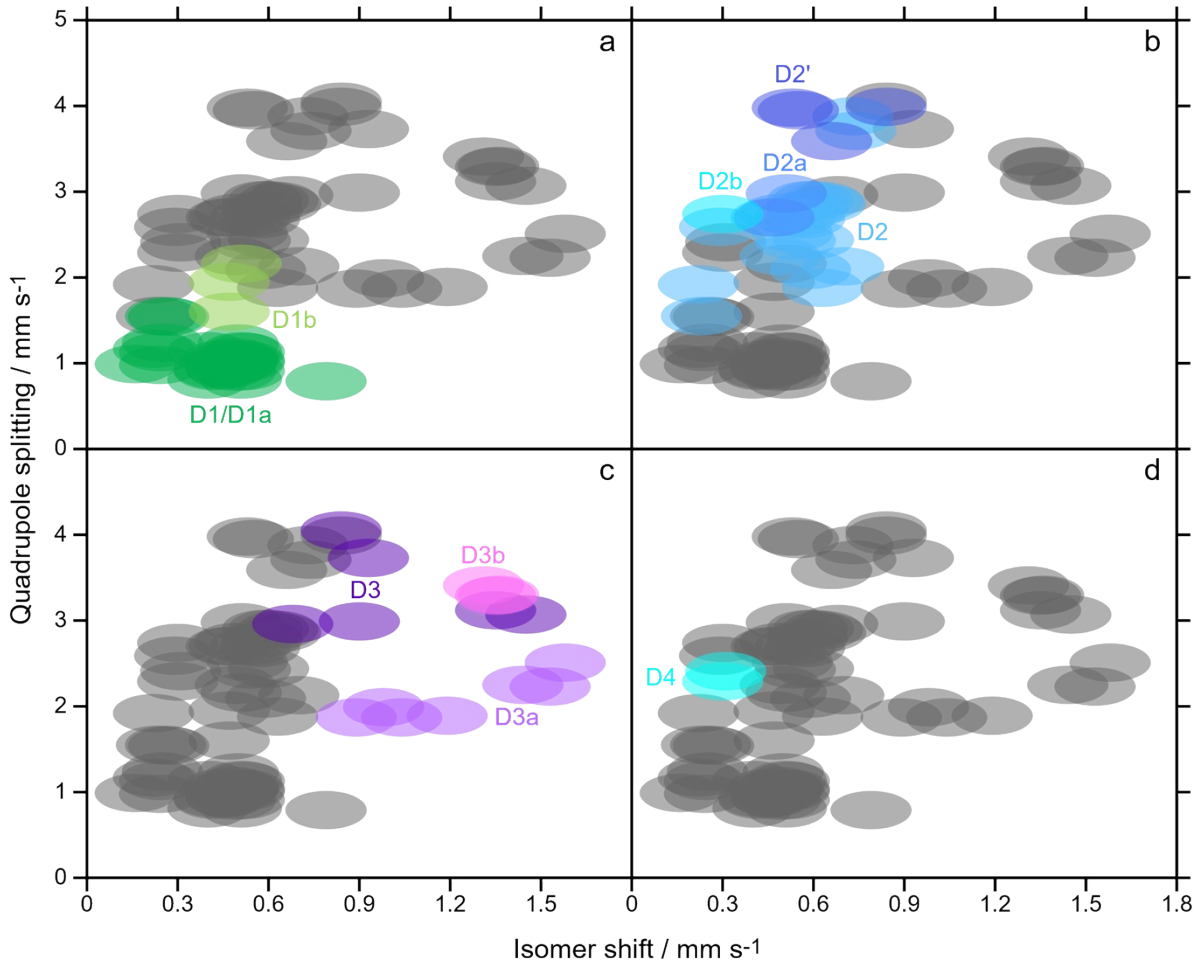

Supplementary Figure S7: Literature low temperature Mössbauer data of FeNC catalysts. Isomer shift and quadrupole splitting values of several Mössbauer doublets measured for FeNC catalysts in the literature are shown. The Mössbauer experiments differ in their conditions and the preparation route of the catalyst, see Supplementary Table S6 for more detail. Only Mössbauer experiments performed at 80 K or below are shown to ensure comparability to quantum chemical calculations. The nomenclature of the doublets follows the assignment in the respective papers. The size of the ellipsoids is chosen to represent the error of calculated Mössbauer parameters as computed in an updated version of the calibration study performed by Gallenkamp *et al.*[1] (±0.13 mm s^{-1} for the isomer shift and ±0.22 mm s^{-1} for the quadrupole splitting).

In panel a, D1/D1a and D1b doublets are highlighted. They are characterized by a low isomer shift and a low, or in case of D1b low to intermediate, quadrupole splitting. While most papers only observe a single D1 doublet behaving like D1a, Ni, Gallenkamp *et al.*[2,3] distinguished between D1a and D1b doublets. It is noteworthy that D1b cannot be observed for electronically activated FeNC catalysts (applied potential below the onset potential).

In panel b, different types of D2 doublets are highlighted. They are characterized by a low to intermediate isomer shift and an intermediate quadrupole splitting. Ni, Gallenkamp *et al.*[2] discern D2a and D2b doublets based on the lower isomer shift of D2b. In contrast to D1a and D1b, only one D2-like doublet appeared per experiment, depending on the preparation route of the catalyst. D2' denotes D2-like doublets observed under *in situ* or *operando* conditions by

Ni, Gallenkamp *et al*.[3] Other literature does not discern D2a, D2b and D2' doublets, therefore the doublets are noted as D2.

In panel c, different types of D3 doublets are highlighted. They show a high isomer shift of usually more than 0.9 mm s^{-1} indicating an iron(II) high-spin system, and an intermediate to high quadrupole splitting. Whereas D1 and D2 doublets are used to fit nearly all experimental Mössbauer spectra, not all works use a D3 doublet. Ni, Gallenkamp *et al.*[2,3] further discerned D3a and D3b doublets, the D3b doublet being characterized by appearing in addition to the D3a doublet under *in situ* conditions for electrically activated catalysts (potential below the onset potential).

In panel d, the so-called "*operando*" doublet D4 is highlighted, which appears only under *operando* conditions. To our knowledge, the work by Ni, Gallenkamp *et al*.[3] contains the only low temperature *operando* Mössbauer experiments published so far and is thus the only work assigning this doublet.

Supplementary Table S6: Low temperature Mössbauer data of FeNC catalysts from the literature. Isomer shift δ_{iso} and quadrupole splitting ΔE_q of the experimental literature doublets shown in Supplementary Figure S7 are listed with the name of the catalyst investigated, the conditions and the temperature T of the Mössbauer experiment, the literature reference and the assignment of the doublet. For the quasi *in situ* measurements, the conditions are given in the form "quasi *in situ*, [applied Potential], [atmosphere], [aged or fresh cathode]".

Doublet	Catalyst	Mössbauer conditions	T / K	δ_{iso} / mm s^{-1}	ΔE_q / mm s^{-1}	Ref.
D1	$Fe_{0.5}$ (not acid leached)	*ex situ*	5	0.51	1.14	4
D1	$Fe_{0.5}$ (not acid leached)	*ex situ*	5	0.48	1.01	4
D1	$Fe_{0.5}$ (not acid leached)	EoT	5	0.49	1.01	4
D1	Fe0.5-NC	*ex situ*	80	0.46	0.94	5
D1	Fe0.5d	*ex situ*	5	0.50	1.03	6
D1	Fe1.0w	*ex situ*	5	0.52	0.91	6
D1	0.1Fe-N-C_m-h+F231t	*ex situ*	10	0.49	0.90	7
D1	0.4Fe-N-C_m-ht	*ex situ*	10	0.46	1.02	7
D1	1.3Fe-N-C_ma-ht	*ex situ*	10	0.49	0.99	7
D1	8.4Fe-N-C_ma-ht	*ex situ*	4.2	0.51	0.81	7
D1	4.7Fe-N-C-ST	*ex situ*	4.2	0.16	0.99	7
D1	1.5Fe-Phen-C	*ex situ*	4.2	0.46	0.93	7
D1	1.2Fe-PANI-C	*ex situ*	4.2	0.50	1.23	7
D1	5.7Fe-N-C-TUB	*ex situ*	4.2	0.52	1.04	7
D1	0.5Fe-N-C-PAJ	*ex situ*	4.2	0.52	1.01	7
D1	0.8Fe-N-C-UB	*ex situ*	4.2	0.79	0.79	7
D1	0.8Fe-N-C-CNRS	*ex situ*	4.2	0.49	1.07	7
D1	NDC-Fe-HT (0 days at atmosphere)	*ex situ*	4.2	0.27	1.54	8
D1	NDC-Fe-HT (2 days at atmosphere)	*ex situ*	4.2	0.25	1.24	8
D1	NDC-Fe-HT (320 days at atmosphere)	*ex situ*	4.2	0.24	1.13	8
D1	$[FeN_4]N_{32}C_{520}$	*ex situ*	4.2	0.22	1.17	9

Doublet	Catalyst	Mössbauer conditions	T / K	δ_{iso} / mm s^{-1}	ΔE_q / mm s^{-1}	Ref.
D1	$[FeN4]_{0.17}[N4]_{0.83}N_{32}C_{520}$	*ex situ*	4.2	0.26	1.55	9
D1	NDC-Fe-HT	*ex situ*	4.2	0.24	0.98	10
D1a	$FeNC_{ppy}$	*ex situ*	1.6	0.45	1.05	2
D1a	$FeNC_{porph}$	*ex situ*	1.6	0.4	1.14	2
D1a	$FeNC_{phen}$	*ex situ*	1.6	0.5	1.04	2
D1a	$FeNC_{phen}$	quasi *in situ*, 900 mV, N_2, aged	1.6	0.42	0.93	3
D1a	$FeNC_{phen}$	quasi *in situ*, 200 mV, N_2, aged	1.6	0.52	1.13	3
D1a	$FeNC_{phen}$	quasi *in situ*, 200 mV, O_2, aged	1.6	0.42	0.91	3
D1a	$FeNC_{phen}$	quasi *in situ*, 200 mV, O_2, fresh	1.6	0.4	0.81	3
D1b	$FeNC_{ppy}$	*ex situ*	1.6	0.47	1.95	2
D1b	$FeNC_{phen}$	*ex situ*	1.6	0.47	1.6	2
D1b	$FeNC_{phen}$	quasi *in situ*, 900 mV, N_2, aged	1.6	0.51	2.16	3
D2	$Fe_{0.5}$ (not acid leached)	*ex situ*, powder	5	0.64	2.86	4
D2	$Fe_{0.5}$ (not acid leached)	*ex situ*, cathode	5	0.49	2.75	4
D2	$Fe_{0.5}$ (not acid leached)	EoT	5	0.46	2.7	4
D2	Fe0.5-NC	*ex situ*	80	0.49	2.25	5
D2	Fe0.5d	*ex situ*	5	0.57	2.68	6
D2	Fe1.0w	*ex situ*	5	0.58	2.79	6
D2	0.4Fe-N-C_m-ht	*ex situ*	10	0.29	2.59	7
D2	1.3Fe-N-C_ma-ht	*ex situ*	10	0.54	2.43	7
D2	4.7Fe-N-C-ST	*ex situ*	4.2	0.23	1.55	7
D2	1.5Fe-Phen-C	*ex situ*	4.2	0.59	2.09	7
D2	1.2Fe-PANI-C	*ex situ*	4.2	0.70	2.13	7
D2	5.7Fe-N-C-TUB	*ex situ*	4.2	0.63	1.88	7
D2	0.5Fe-N-C-PAJ	*ex situ*	4.2	0.53	2.52	7
D2	0.8Fe-N-C-UB	*ex situ*	4.2	0.60	2.44	7
D2	0.8Fe-N-C-CNRS	*ex situ*	4.2	0.54	2.70	7
D2	NDC-Fe-HT (0 days at atmosphere)	*ex situ*	4.2	0.63	2.89	8
D2	NDC-Fe-HT (2 days at atmosphere)	*ex situ*	4.2	0.60	2.90	8
D2	NDC-Fe-HT (320 days at atmosphere)	*ex situ*	4.2	0.58	2.90	8
D2	$[FeN_4]N_{32}C_{520}$	*ex situ*	4.2	0.74	3.71	9
D2	$[FeN4]_{0.17}[N4]_{0.83}N_{32}C_{520}$	*ex situ*	4.2	0.73	3.88	9
D2	NDC-Fe-HT	*ex situ*	4.2	0.22	1.92	10
D2'	$FeNC_{phen}$	quasi *in situ*, 900 mV, N_2, aged	1.6	0.84	3.99	3
D2'	$FeNC_{phen}$	quasi *in situ*, 200 mV, N_2, aged	1.6	0.66	3.59	3

Doublet	Catalyst	Mössbauer conditions	T / K	δ_{iso} / mm s^{-1}	ΔE_q / mm s^{-1}	Ref.
D2'	$FeNC_{phen}$	quasi *in situ*, 200 mV, O_2, aged	1.6	0.53	3.98	3
D2'	$FeNC_{phen}$	quasi *in situ*, 200 mV, O_2, fresh	1.6	0.55	3.95	3
D2a	$FeNC_{ppy}$	*ex situ*	1.6	0.51	2.98	2
D2a	$FeNC_{phen}$	*ex situ*	1.6	0.47	2.7	2
D2b	$FeNC_{porph}$	*ex situ*	1.6	0.3	2.74	2
D3	$Fe_{0.5}$ (not acid leached)	EoT	5	1.35	3.12	4
D3	0.1Fe-N-C_m-h	*ex situ*	10	0.84	4.05	7
D3	0.4Fe-N-C_m-ht	*ex situ*	10	1.45	3.07	7
D3	1.3Fe-N-C_ma-ht	*ex situ*	10	0.93	3.73	7
D3	4.7Fe-N-C-ST	*ex situ*	4.2	0.68	2.96	7
D3	NDC-Fe-HT	*ex situ*	4.2	0.90	2.99	10
D3a	$FeNC_{ppy}$	*ex situ*	1.6	1.58	2.51	2
D3a	$FeNC_{porph}$	*ex situ*	1.6	1.53	2.23	2
D3a	$FeNC_{phen}$	*ex situ*	1.6	1.44	2.25	2
D3a	$FeNC_{phen}$	quasi *in situ*, 900 mV, N_2, aged	1.6	1.19	1.89	3
D3a	$FeNC_{phen}$	quasi *in situ*, 200 mV, N_2, aged	1.6	0.89	1.87	3
D3a	$FeNC_{phen}$	quasi *in situ*, 200 mV, O_2, aged	1.6	1.04	1.87	3
D3a	$FeNC_{phen}$	quasi *in situ*, 200 mV, O_2, fresh	1.6	0.98	1.99	3
D3b	$FeNC_{phen}$	quasi *in situ*, 200 mV, N_2, aged	1.6	1.36	3.3	3
D3b	$FeNC_{phen}$	quasi *in situ*, 200 mV, O_2, aged	1.6	1.31	3.41	3
D3b	$FeNC_{phen}$	quasi *in situ*, 200 mV, O_2, fresh	1.6	1.35	3.29	3
D4	$FeNC_{phen}$	quasi *in situ*, 200 mV, O_2, aged	1.6	0.31	2.41	3
D4	$FeNC_{phen}$	quasi *in situ*, 200 mV, O_2, fresh	1.6	0.3	2.29	3

- Comparison of Single Point Calculation Protocols -

Supplementary Table S7: Energies and Mulliken spin population on iron of model 3 with different calculation protocols. The final single point energy (FSPE), the relative spin state energy E_{Rel} and the Mulliken spin population on the iron atom of model **3** calculated with two different single point calculation protocols are shown. The first protocol uses the OLYP functional and ORCA version 4.2, the second one uses the OPBE functional and ORCA version 5.0, otherwise, they are identical. As one can see, the multiplicity of the electronic ground state remains the same for both protocols.

		Single Point (OLYP, ORCA 4.2)			**Single Point (OPBE, ORCA 5.0)**		
	M	***FSPE* / Ha**	**E_{Rel} / kcal mol^{-1}**	**Mull (Fe)**	***FSPE* / Ha**	**E_{Rel} / kcal mol^{-1}**	**Mull (Fe)**
3	1	-3399.3287	36.5	0.00	-3399.1710	15.8	0.00
	3[a]	-3399.3870	0.0	1.88	-3399.1962	0.0	2.30
	5	-3399.3614	16.0	2.67	-3399.1734	14.3	2.75
3 (extended)	1	-5003.6723	64.8	0.00	-5003.4519	15.6	0.00
	3	-5003.7756	0.0	1.86	-5003.4768	0.0	2.35
	5	-5003.7091	41.7	3.75	-5003.4598	10.7	2.76
3*O2 (end-on)	1	-3549.7618	4.9	0.00	-3549.5220	5.8	0.00
	3	-3549.7675	1.4	2.00	-3549.5279	2.1	2.09
	5	-3549.7697	0.0	2.52	-3549.5313	0.0	2.59
(side-on)	1	-3549.7655	2.6	0.00	-3549.5295	1.1	0.00
	3	-3549.7645	3.3	1.77	-3549.5289	1.5	1.82
	5	-3549.7654	2.7	2.63	-3549.5290	1.4	2.67
3*OH	2	-3475.2125	15.4	0.92	-3474.9982	17.1	0.96
	4	-3475.2370	0.1	2.68	-3475.0235	1.2	2.74
	6	-3475.2371	0.0	4.14	-3475.0255	0.0	4.22
3*H2O	1	-3475.8036	15.1	0.00	-3475.5975	21.9	0.00
	3	-3475.8276	0.0	2.24	-3475.6325	0.0	2.29
	5	-3475.8275	0.1	3.80	-3475.6249	4.8	3.87
	5	-3475.8168	6.8	2.70	-3475.6162	10.2	2.79
3*2 H2O	1	-3552.2577	0.8	0.00	-3552.0438	1.6	0.00
	3	-3552.2343	15.5	0.82	-3552.0230	14.6	0.89
	5	-3552.2590	0.0	2.72	-3552.0463	0.0	2.82

[a] The single point calculations of the two calculation protocols yield different orbital occupations for this state, leading to the difference in the Mulliken spin population. This, however, is not viewed any further, as for these systems a multireference character is expected.

- Supplementary Files -

Supplementary Files "geometries.zip": Geometry files of the models used in this work. In the attached .zip-folder "geometries.zip", the geometries of all models investigated in this work can be found as .xyz-files. The geometries given are those obtained from the TPSS geometry optimizations. The files are named following the scheme "{Model}-{Ligand}[_{Specifications}]_c{charge}m{2S+1}.xyz". In the first line of each file, the number of atoms is given, in the second line the name of the model as "{Model}-{Ligand} [({specifications})], 2S+1 = {2S+1}" together with the models final single point energy (FSPE) in Hartree according to the OPBE/OLYP-single point calculation.

Note that no .xyz-file of $\mathbf{1}_{Large}$ in the LS state is given, as no energetic minimum could be obtained during geometry optimization. Also note, that for the structure of $\mathbf{2}_{Large}$, no frequency calculation could be performed and thus it could not be confirmed, that the structure is indeed an energetic minimum.

- References -

(1) Gallenkamp, C.; Kramm, U. I.; Proppe, J.; Krewald, V., Calibration of computational Mössbauer spectroscopy to unravel active sites in FeNC catalysts for the oxygen reduction reaction, *International Journal of Quantum Chemistry*; **2021**, *121*; DOI: 10.1002/qua.26394.

(2) Ni, L.; Gallenkamp, C.; Paul, S.; Kübler, M.; Theis, P.; Chabbra, S.; Hofmann, K.; Bill, E.; Schnegg, A.; Albert, B.*; et al.*, Active Site Identification in FeNC Catalysts and Their Assignment to the Oxygen Reduction Reaction Pathway by In Situ 57 Fe Mössbauer Spectroscopy, *Advanced Energy and Sustainability Research*; **2021**, *2*; DOI: 10.1002/aesr.202000064.

(3) Ni, L.; Gallenkamp, C.; Wagner, S.; Bill, E.; Krewald, V.; Kramm, U. I., Identification of the Catalytically Dominant Iron Environment in Iron- and Nitrogen-Doped Carbon Catalysts for the Oxygen Reduction Reaction, *Journal of the American Chemical Society*; **2022**, *144*, 16827–16840; DOI: 10.1021/jacs.2c04865.

(4) Li, J.; Sougrati, M. T.; Zitolo, A.; Ablett, J. M.; Oğuz, I. C.; Mineva, T.; Matanovic, I.; Atanassov, P.; Huang, Y.; Zenyuk, I.*; et al.*, Identification of durable and non-durable FeNx sites in Fe–N–C materials for proton exchange membrane fuel cells, *Nature Catalysis*; **2021**, *4*, 10–19; DOI: 10.1038/s41929-020-00545-2.

(5) Mineva, T.; Matanovic, I.; Atanassov, P.; Sougrati, M.-T.; Stievano, L.; Clémancey, M.; Kochem, A.; Latour, J.-M.; Jaouen, F., Understanding Active Sites in Pyrolyzed Fe–N–C Catalysts for Fuel Cell Cathodes by Bridging Density Functional Theory Calculations and 57 Fe Mössbauer Spectroscopy, *ACS Catalysis*; **2019**, *9*, 9359–9371; DOI: 10.1021/acscatal.9b02586.

(6) Sougrati, M. T.; Goellner, V.; Schuppert, A. K.; Stievano, L.; Jaouen, F., Probing active sites in iron-based catalysts for oxygen electro-reduction: A temperature-dependent 57 Fe Mössbauer spectroscopy study, *Catalysis Today*; **2016**, *262*, 110–120; DOI: 10.1016/j.cattod.2015.10.017.

(7) Bates, J. S.; Martinez, J. J.; Hall, M. N.; Al-Omari, A. A.; Murphy, E.; Zeng, Y.; Luo, F.; Primbs, M.; Menga, D.; Bibent, N.*; et al.*, Chemical Kinetic Method for Active-Site Quantification in Fe-N-C Catalysts and Correlation with Molecular Probe and Spectroscopic Site-Counting Methods, *Journal of the American Chemical Society*; **2023**, *145*, 26222–26237; DOI: 10.1021/jacs.3c08790.

(8) Menga, D.; Wagner, F. E.; Fellinger, T.-P., Life cycle of single atom catalysts: a Mössbauer study on degradation and reactivation of tetrapyrrolic Fe-N-C powders, *Materials horizons*; **2023**, *10*, 5577–5583; DOI: 10.1039/D3MH00308F.

(9) Menga, D.; Guilherme Buzanich, A.; Wagner, F.; Fellinger, T.-P., Evaluation of the Specific Activity of M-N-Cs and the Intrinsic Activity of Tetrapyrrolic FeN4 Sites for the Oxygen Reduction Reaction, *Angewandte Chemie (International ed. in English)*; **2022**, *61*, e202207089; DOI: 10.1002/anie.202207089.

(10) Menga, D.; Low, J. L.; Li, Y.-S.; Arčon, I.; Koyutürk, B.; Wagner, F.; Ruiz-Zepeda, F.; Gaberšček, M.; Paulus, B.; Fellinger, T.-P., Resolving the Dilemma of Fe-N-C Catalysts by the Selective Synthesis of Tetrapyrrolic Active Sites via an Imprinting Strategy, *Journal of the American Chemical Society*; **2021**, *143*, 18010–18019; DOI: 10.1021/jacs.1c04884.